

# Thesis Title

Thesis Subtitle

**CHAN, Yan-Chak Christopher**

**Supervised by:**

Prof. Dr. Hannes Taubenöck <sup>1</sup>  
Emran Alchikh Alnajar <sup>2</sup>

Masterarbeit submitted for the degree of  
Master der Naturwissenschaften  
in

Applied Earth Observation and Geoanalysis of the Living  
Environment (EAGLE)



Philosophische Fakultät (Historische, Philologische, Kultur- und  
Geographische Wissenschaften)  
Julius-Maximilians-Universität Würzburg

## **Forewords and Acknowledgements**

## **Declaration of Independent Work**

## **Figure list**

## **Abbreviations**

## **Abstract**

  Lorem ipsum dolor sit amet, consectetur adipiscing elit. Curabitur dignissim, quam maximus posuere cursus, magna justo rutrum erat, at mattis magna magna nec risus. Duis lacus lectus, condimentum a viverra eu, fermentum molestie lorem. Sed maximus, enim eu scelerisque dictum, sem erat mollis massa, in dictum ante libero a tortor. Cras nulla nisi, sollicitudin ac suscipit cursus, maximus non dui. Sed venenatis ligula id efficit imperdiet. Vivamus ut magna eleifend, rutrum ante facilisis, pulvinar turpis. Maecenas at interdum lorem. Duis vel varius ligula. Sed magna erat, egestas vitae varius id, cursus vitae neque. Orci varius natoque penatibus et magnis dis parturient montes, nascetur ridiculus mus. Phasellus interdum lectus mi, a dapibus lorem tristique a. Phasellus molestie vestibulum metus a fringilla. Pellentesque at rhoncus nulla. Praesent posuere turpis nec leo fringilla egestas.

  Pellentesque auctor vel dolor eu viverra. Ut faucibus nunc orci, eu aliquam justo hendrerit vel. Proin auctor sed nisl non posuere. Vivamus orci orci, commodo eget semper nec, tempus at arcu. Nam eget leo cursus velit aliquam varius. Curabitur nisi dui, rutrum vitae elit a, mollis volutpat mauris. Suspendisse potenti. Nam convallis magna iaculis posuere aliquam. Quisque tristique rutrum placerat. Quisque ultricies molestie lacinia. Maecenas at nisi in neque dictum consequat.

# *Contents*

0.1	Forewords and Acknowledgements . . . . .	ii
0.2	Declaration of Independent Work . . . . .	iii
0.3	Figure list . . . . .	iv
0.4	Abbreviations . . . . .	v
<b>1</b>	<b>Introduction</b>	<b>3</b>
1.1	Study Area of Interest . . . . .	5
1.1.1	Kalobeyei, Kakuma, Turkana, Kenya . . . . .	5
1.1.2	Dzaleka, Dowa, Malawi . . . . .	6
<b>2</b>	<b>Literature Review</b>	<b>9</b>
2.1	Remote Sensing of Informal Settlements . . . . .	9
2.2	Deep Learning in Urban Remote Sensing . . . . .	10
2.2.1	Computer Vision and a brief review of Convolutional Neural Networks . . . . .	10
2.2.2	UAV-based informal settlement segmentation . . . . .	11
2.2.3	Fundamentals of Deep Learning and Convolutional Neural Networks . . . . .	12
<b>3</b>	<b>Data and Methodologies</b>	<b>17</b>
3.1	Data . . . . .	17
3.1.1	Raster pre-processing . . . . .	17
3.1.2	Data Augmentation . . . . .	17
3.2	Research Questions and experiment design . . . . .	18
3.3	Architecture and hyperparameter selection . . . . .	19
3.3.1	The U-Net and U-Net variants . . . . .	19
3.3.2	Pre-trained weights on Deep Learning models . . . . .	19
3.4	Accuracy Assessment . . . . .	19
3.4.1	Precision, Recall, Sensitivity, and Specificity . . . . .	20
3.4.2	Overall Accuracy, Dice Score, and Intersection-over-Union . . . . .	22
3.5	Experimentation setup . . . . .	22
3.5.1	Project workflow . . . . .	22

<b>4</b>	<b>Findings</b>	<b>23</b>
4.1	Analysis . . . . .	23
<b>5</b>	<b>Discussion</b>	<b>24</b>
<b>6</b>	<b>Conclusion</b>	<b>25</b>
<b>7</b>	<b>Bibliography</b>	<b>26</b>
<b>A</b>	<b>Appendix</b>	<b>27</b>

# *Introduction*

The world's population is more urbanised than ever before. As of 2018, approximately 4 billion (55%) (UN DESA., 2018, Taubenöck et al., 2009) reside in urban areas, of which 60% reside in slums often located at the fringes of the city (Venables A., 2018). Urbanisation growth is expect to increase by 2.5 billions between 2018 to 2050, most of which will be in Asia and Africa (UN DESA., 2018). When population growth outpace development, slums became the supplier of significant housing stocks. These informal settlements are dynamic and represent a good reflection of cultural practices, access to resources, financial limitations and other socio-economic conditions. This means the informal settlement differs significantly between urban and rural settlements of roof covers, densities, and are subjected to different levels of access to resources and the types of resources.

Refugee camps are often the common or only way for displaced people to receive shelters and assistance. They are often setup in place of proximity to displaced population, whether that be from natural disasters, human caused disasters, or other reasons. Throughout history, refugee sites have provided haven to the world's most vulnerable population (UN, 2018, Turner S., 2016, UNHCR, 2021). However as of 2020, out of the 26.4 million refugees, only around 1.4 million have access to third country solution between 2016 to 2021 (UNHCR, 2021). Additionally, although officially defined as temporary settlement, many refugee camps have had longer than expected life cycle, some of them have even became "Secondary Cities" and therefore suffers similar problems of poor governance and rapid urbanisation which consequentially makes them unattractive as investment (Cities Alliance & AfDB., 2022). For the many refugee camps and informal settlements that have lasted well beyond their expected temporary role, there are in generally 3 ways of solving the issue: 1. Voluntary repatriation, 2. Reolocation to third country, 3. Local integration as outlined by the Global Compact on Refugees (UN, 2018), although actual implementations are often subjected to the wills of the host sovereign-state. Recent studies have suggested that local integration often have a net positive economical impact on the surrounding region (Alix-Garcia et al., 2018, Rummery A., 2019, IFC., 2018).

The United Nations Department of Economic and Social Affairs have set out a set of 17 Sustainable Development Goals (herein SDG) to be achieved as of 2030 (UN, 2015). Special attention are drawn to Goals 1 and 10 that are particularly relevant, of which this study hope to contribute to.

- *Goal 1: End poverty in all its forms everywhere*
  - *Target 1.1: By 2030, eradicate extreme poverty for all people everywhere, currently measured as people living on less than \$1.25 a day*
  - *Target 1.4: By 2030, ensure that all men and women, in particular the poor and the vulnerable, have equal rights to economic resources, as well as access to basic services, ownership and control over land and other forms of property, inheritance, natural resources, appropriate new technology and financial services, including microfinance*
  - *Target 1.b: Create sound policy frameworks at the national, regional and international levels, based on pro-poor and gender-sensitive development strategies, to support accelerated investment in poverty eradication actions*
- *Goal 10: Reduce inequality within and among countries*
  - *Target 10.1: By 2030, empower and promote the social, economic and political inclusion of all, irrespective of age, sex, disability, race, ethnicity, origin, religion or economic or other status*
  - *Target 10.7: Facilitate orderly, safe, regular and responsible migration and mobility of people, including through the implementation of planned and well-managed migration policies*

Thus, the overarching theme of this thesis is about reducing the geospatial data inequality of informal settlements (Herfort et al., 2021), thereby to improve future decision making in both humanitarian and non-humanitarian context. As the topic and data provider of this project, the Humanitarian OpenStreetMap (herein HOTOSM) have been at the forefront of using open and crowd sourced mapping data to support humanitarian causes from shorter term disaster response to longer epidemiology and microfinance campaigns (HOTOSM, 2021). Having up-to-date map is therefore paramount for short and long term humanitarian projects, and with the advent of Deep Learning in the last decade, AI-assisted mapping have became a major topic for innovation (e.g. Herfort et al., 2019, Kuffer et al., 2016, Wurm et al., 2021, Quinn et al., 2018).

## **Study Area of Interest**

### **Kalobeyei, Kakuma, Turkana, Kenya**

The Kakuma camp was first established in 1992, located in the North-West of Kenya in Turkana County. The camp was initially established to provide accommodation to the refugees fleeing the Second Sudanese Civil War as a temporary solution. However, as the conflict became drag out and followed by subsequent conflicts in the nearby region, the Kakuma camp have therefore been running for the past 30 years. As of 2020, Kakuma is home to 157,718 refugees with increasing number coming from the more recent Somali and Ethiopian-Eritrean conflict (IFC., 2018, UN-HABITAT, 2021). The Kalobeyei Integrated Settlement established in 2015 benefited from a much better spatial planning in order to facilitate inclusive socio-economic development (UN-HABITAT, 2021, UNHCR & DANIDA, 2019) (*see figure 1.1*).

The Kakuma refugee camp have fluctuated in population as a response to demand, however, a dramatic increase in population in 2013 to 2014 has culminated into the development of Kakuma 4 Camp and the Kalobeyei Settlement and the Kalobeyei Integrated Socio-Economic Development Plan (KISEDP) which is the local integration strategies. Both the Kakuma and Kalobeyei refugee camps have local integration as the targeted solution (UN-HABITAT, 2021, UNHCR & DANIDA, 2019). A comprehensive study of the formal and informal economy of Kakuma refugee camp conducted by the International Financial Corporation (IFC, 2018) suggests that that market catering for the refugees and surrounding towns is estimated at KES 1.7 billion (USD \$16.4 million). The economical vibrancy of local integration have improve significantly the impoverished Turkana county. However, challenges remain in integration into the wider Kenyan economy.

### **Dzaleka, Dowa, Malawi**

Originally an infamous prison camp under the Banda's Malawi Congree Party regime, the area was converted to become the Dzaleka Refugee Camp in 1994. Unlike the Kakuman and Kalobeyei camp, the Dzaleka Refugee Camp is located in the heart of Malawi, 45 km away from the capital Li-longwe, where it is home to around 52,000 refugees and receive on average 300 new residents every month. Most coming from the Great Lakes area, in particular, the Democratic Republic of Congo and Burundi. However, resurgence of past conflicts between the Republic of Congo and D.R. Congo have caused an increased of influx in recent years (UNHCR, 2014, Kaval E., 2016). Much of the infrastructure in the Dzaleka camp infrastructures remain in rudimentary at best, and very little resources and statistics were available via the UNHCR and UNDP portals. The Northern extension to the Dzaleka main camp is known as the Katubza extension (*referred to as Dzaleka North by the rest of this thesis*), it is a well-planned plot of land consisting of 423 shelter shelters and were still inconstruction as of March 2021 (Gross G., 2021 & UNHCR, 2021) (*see figure 1.2*).

Although hosting of refugee camps are often seen as a burden on the surface level, in reality, many refugees are often more educated than the local population, which brings with them entrepreneurial ability and provide the local-area with extra labour force (Alix-Garcia et al., 2018). )With constant stakeholder pressure for relocation and closure, showcasing of the refugee camps local economic impact and the potentialof stimulating previously impoverished area could make the case for their remain (Cities Alliance, 2022).

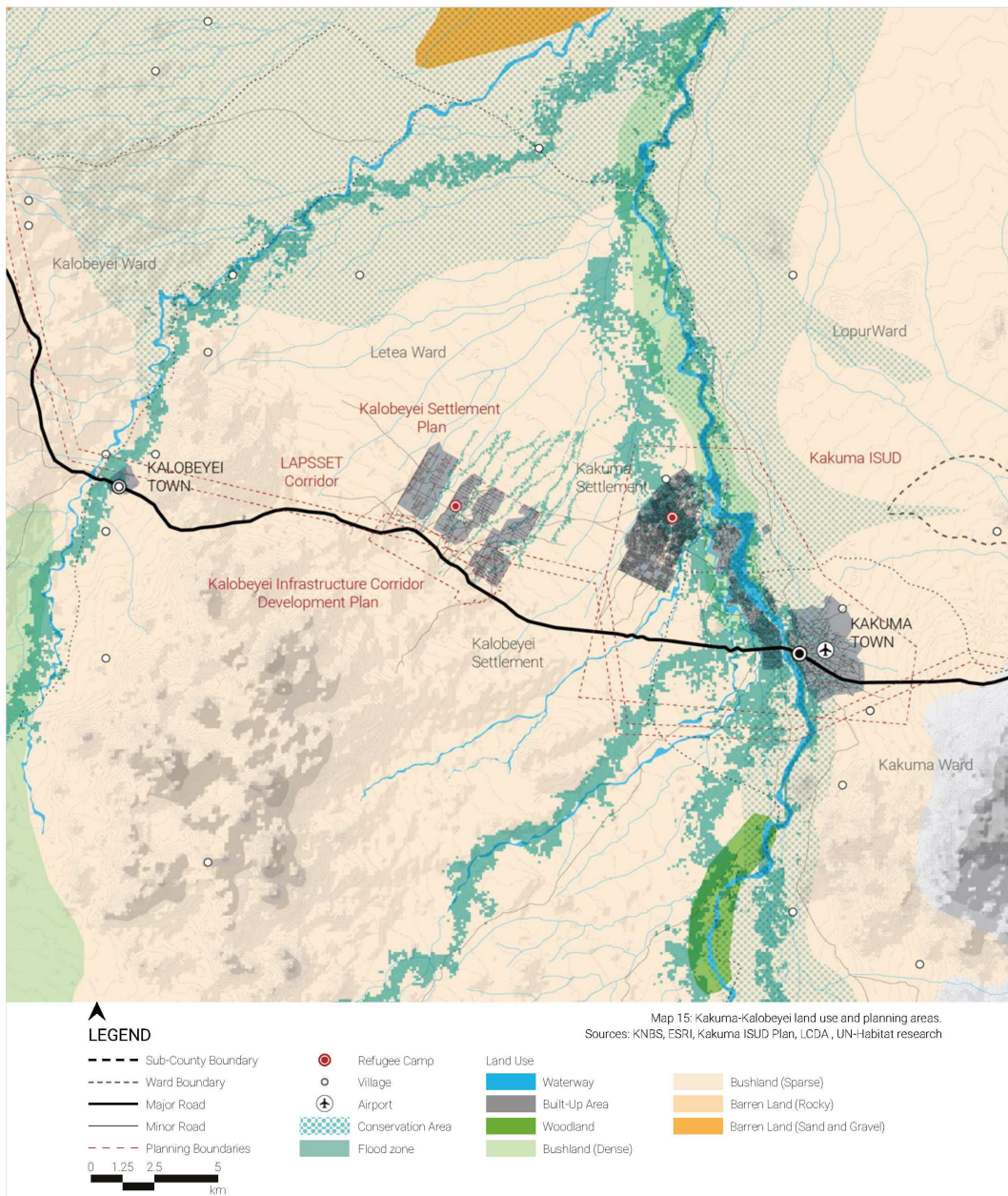


Figure 1.1: The Kakuma-Kalobeyei land use and planning areas (UN-HABITAT, 2018)

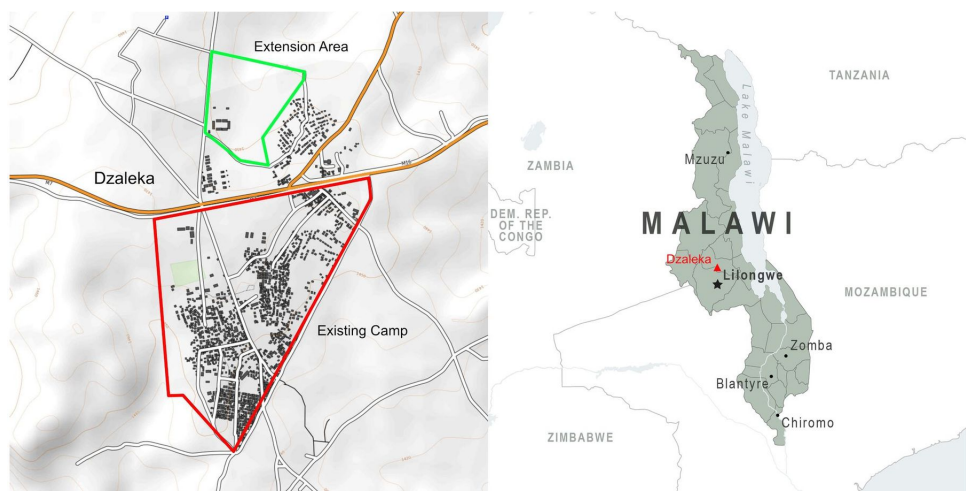


Figure 1.2: The main Dzaleka Refugee Camp and the Katubza extension plan (Dzaleka North) designed by Urban Design Advisor to the UNHCR Werner Schnellenberg (Gerhard G., 2021).

# *Literature Review*

## **Remote Sensing of Informal Settlements**

Remote sensing of the urban environments have always been the unorthodox in remote sensing, but simultaneously, it is the topic that essentially funded many long-standing satellite programs such as the Landsat and SPOT programs. The complexity of human built environments often consist of using very different materials in conjunction to each other in a dense environment. From power-lines, factories, car-park, to leisure-parks, imaging of urban environments therefore requires data high in both spatial and temporal resolution and often employs techniques that extracts geometry, textural, and other physical features as oppose to the more common spectral based index approach used in ecological or environmental remote sensing (Jensen J., 2007, NRC., 1998). Higher granularity urban remote sensing have until very recently remained in the monopoly of defense and reconnaissance services.

Informal settlement and slums mapping of developing countries require very high resolution (VHR) images which was unavailable until the turn of the century. The relatively new technology thus only began to gain traction within the last 2 decades. Particularly with the increase in the availability of VHR satellites. Increase in computational power had enabled novel techniques such as multi-layer machine learning, textural analysis, and novel geostatistical methods to emerge (Kuffer et al., 2016). Due to frequent repeat coverage of satellite's orbit, they can be used to fill in between periodic census that are costly and time consuming to conduct. Census also does not do a good job in capturing larger scale units and spatial patterns, potentially overlooking others socioeconomic determinants such as cropping cycles and infrastructure access etc. Availability of VHR sensors and publications on slums and remote sensing (Kuffer et al., 2016). Remote sensing of settlements largely falls under 2 categories, rural or urban. Due to the different make-up of socioeconomic context and urban morphology, sensing rural and urban settlements require different parameters. Additionally, there's no "one size fit all" way to generalise informal and formal settlement across the

world, as physical geography, topography, cultural, and available resources often dictate the distribution, development, and settlement clusters pattern. These unique requirements have thus made deep learning techniques particularly useful, and many application of deep learning in remote sensing have therefore been in the urban domain (Ma et al., 2019).

## Deep Learning in Urban Remote Sensing

The following section will be divided into 3 parts. The first part reviews the concept of Computer Vision as a study subject, previous common practice, and the evolution towards data-driven Deep Learning. The second part will focus on domain specific review of recent AI-based segmentation practices on building segmentation and particularly the recent practices in informal settlement segmentation. Lastly, the third part will explain the mechanism of the Convolutional Neural Network, the class of neural networks commonly used for CV tasksj

### Computer Vision and a brief review of Convolutional Neural Networks

Prior to the paradigm shift towards data-driven and ML based segmentation techniques, image segmentation were performed manually with the aid of a few algorithms (Pal & Pal, 1993). The image segmentation tasks often starts with acquiring less-noisy imagery or data, this is followed by applying multitudes of CV based edge detector (e.g. Sobel, Prewitt, Marr-Hildreth) or Grey-Level Co-occurrence Matrix kernel (e.g. Haralich Texture) (e.g. Kuffer et al., 2014, kuffer et al., 2016, Wurm et al., 2017). This can be considered to be the pre-processing steps necessary to extract information to select the parameters for the segmentation algorithms. (Pal & Pal, 1993, Blaschke T., 2010, Blaschke et al., 2014). The field of computer-vision based segmentation experienced an akin to a Kuhnian paradigm shift (Kuhn T., 1962) when Krizhevsky et al. (2012) AlexNet won the ImageNet challenge, it reinvigorated the use of multi-layered neural network in Computer Vision tasks (LeCun et al., 2015). The timing of the paradigm shift coincided with the increase in computation power provided by Graphical Processing Unit (GPU) have enabled CNNs to be successfully applied across domains ranging from biomedical imaging to remote sensing (Ma et al., 2018, Zhu et al., 2017, Zhang et al., 2016, Wurm et al., 2019).

In the field of Computer Vision, there is generally 4 types of application: 1. Semantic segmentation, 2. Classification and localisation, 3. Object detection, and 4. Instance segmentation (*see figure ??*) (Stevens et al., 2020). This study will conduct semantic segmentation of binary class between built-up and no built-up.

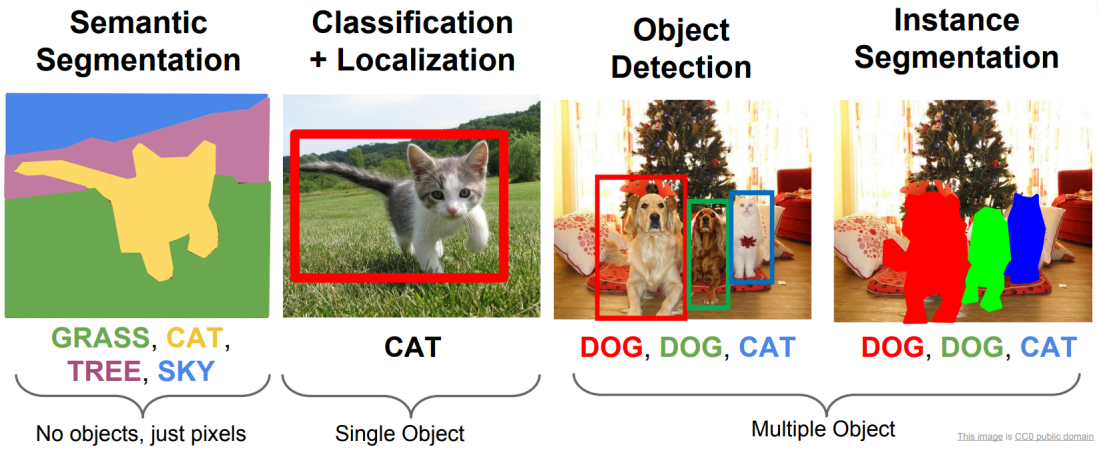


Figure 2.1: The four main types of Computer Vision tasks (Stanford University, 2022)

The purpose of semantic segmentation is to assign a specific named (semantic) classification to each and every single pixel of the input image. This is commonly applied in remote sensing of Land Use Land Cover classification where every single pixel will be assigned a Land Cover or Land Use type. Another application is binary segmentation where the model will only be trained to assign a named classification to a particular cluster of associated pixels. This is more common in single class segmentation. The difference between mere classification and segmentation is that the semantic segmentation output a mask over the pixel will be created, where each pixel within the mask belongs to the same semantic task; meanwhile, classification only gives a confidence of semantic of the whole scene without assigning the classification to each pixel.

### UAV-based informal settlement segmentation

The advent of orthorectified photos from Surface-from-Motion have drastically democratised the collection of VHR imagery. Not only are UAV images extremely economical to procure, the spatial resolution for informal settlement application could only be rivaled by perhaps the best reconnaissance or commercial satellite which is either difficult or very expensive to obtain. ,

The issue with any Deep Learning Project is the high amount of data required (Tan et al., 2018, )

## Fundamentals of Deep Learning and Convolutional Neural Networks

Prior to the resurgence of popularity in DL, the set of methodology associated was known as a multi-layered perceptron. Initially inspired by a mathematical analogy to codified the function of a single neuron. The seminal Psychological review paper published by Rosenblatt F, (1958). Like a human neuron, The properties of a perceptron ont he most fundamental level takes an information/numerical input, stores and apply transformation, and create an output. Through stacking of basic perceptrons, a multi-layered perceptrons structure can be created. In order for such structure to be computationally useful, it must satisfy the following criteria:

1. Collections of connected perceptrons are capable of plasticity (i.e. changing values) through training.
2. Perceptrons will form dominant pathways that "fire" (activate) together.
3. Through training, perceptrons will learn to apply positive or negative reinforcement to facilitate minimising error (e.g. assigning and changing "weights").

The particular group of such perceptron structures used in CVs are known as Convolutional Neural Network (herein CNN) The most basics of the CNN consist of 3 parts: 1. A hidden layer, 2. Multiple hidden convolution and pool layers, 3. An output layer which provides with the segmentation result and the associated confidence level (*see figure: 2.2 2.3*). Therefore, a Deep-Learning Neural Network system is string together by an series of inter-connected layer of which its parameters are adjustable to adapt to the data provided to it. Through careful iterative training and adjustment, the system can generalise well not only to the training and validation data, but to future datasets as well.

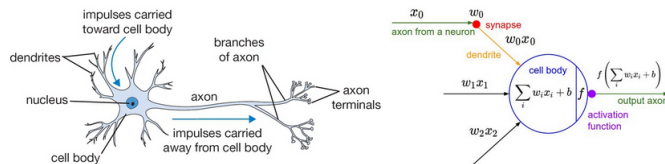


Figure 2.2: Schematic analogy diagram between a biological neuron and an artificial perceptron (Fumo D., 2017).

$$f\left(\sum_{i \dots n} w_i x_i + b\right)$$

- Where:
  - $f$  = Activation function
  - $\sum(i \dots n)$  = Summation of i to nth dimension
  - $w_i x_i$  = weights multiplied by original input variable ( $x$ )
  - $b$  = bias

(2.1)

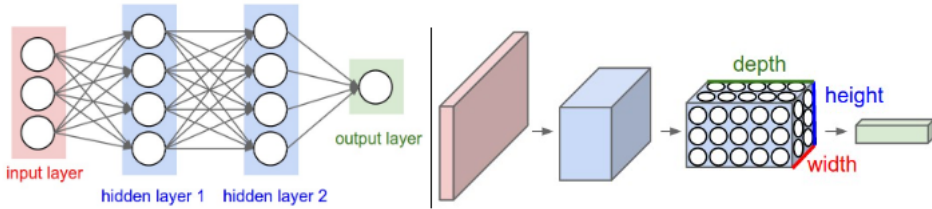


Figure 2.3: Schematic diagram of a CNN (Stanford University, 2022).

### Convolution and Pooling

The hidden layers of the CNN is where the network performs representation learning, where with each depth layer learns more abstract features of the inputted training image. While not often the case, it is conventional practice to interleave the convolutional and the pooling layers (Stevens et al., 2020). The convolutional layer employs a sliding kernel which applies the weighted filter as displayed in [2.2.3](#)

The convolutional layer is essentially treats every image pixel as vector in a 3-Dimensional layout with input of  $(BatchSize, Channel_{in}, Height, Width)$ , the convolutional kernel slides and apply the weighting and bias terms to extract deeper features (Stevens et al., 2020), thus, learning more deeper features which creates the output of  $(BatchSize, Channel_{out}, Height, Width)$ . The full transformation per convolutional layer transform *equation:* [2.2.3](#) of each pixel into *equation:* [2.2.3](#):

$$out(N_i, C_{outj}) = bias(C_{outj}) + \sum_{k=0}^{C_{in}-1} weight(C_{outj}, k) * input(N_i, k)$$

- Where:

- $N$  = Batch Size
- $C$  = Channels
- $k$  = Kernel Size
- \*Further details can be found in [PyTorch documentation for nn.Conv2d](#)

(2.2)

The pooling layer reduces the dimension by downsampling by applying conventionally, a smaller kernel which extract the desirable value when applied. Maximum Pooling, which only retains the largest value in the downsampling kernel is common and is used for the network architecture of this experiment (Stevens et al., 2020). The pooling layer should scale down the image while retaining the most crucial information *see figure: 2.4.*

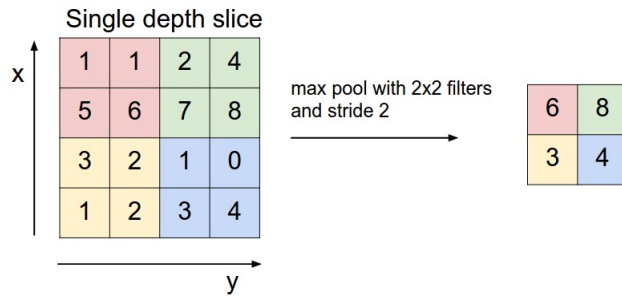


Figure 2.4: Max pooling (Stanford University, 2022).

### Optimiser and the Binary Cross Entropy Loss function

With each complete pass through the neural network, the ouput is then compared against the validation result for error calculation. The summed average of loss thus defines the cost function landscape from which the error value is calculated against, penalising when prediction is incorrect and rewarding if otherwise. This enables backpropagation and the adjustments of the weights and biases in the proceeding pass. Due to the binary segmentation task for this study, the Binary Cross Entropy loss function was used to measure error *equation: 2.2.3.*

$$l(x, y) = L = \{l_1 \dots l_N\}^T, l_n = -w_n[y_n * \log x_n + (1 - y_n) * \log(1 - x_n)]$$

- Where:

- $N$  = Batch Size
- $l(x, y)$  = loss(Probability, Binary Classification)
- $l_n$  = loss at sample  $n$
- \*Further details can be found in [PyTorch documentation for nn.BCELoss](#)

(2.3)

The optimiser controls the gradient descent, a suitable optimiser prevents gradient descent to be trapped at a local minimum in the cost landscape. The optimiser of choice for the experiment is the Adam optimiser, the specific and technical aspects will be further discussed in section [3.3](#).

### Backpropagation and the chain rule

In order for a neural network to improve, the weights and bias are changed accordingly to minimisation of the cost function. This is computed as a step-wise function as a negative vector against the cost landscape. Which each parameter of the weights and biases of each neuron within the neural network is defined as a chained function against the cost in *equation: 2.2.3*. In other words, what is the derivate of the cost function with respect to the chain of weights and biases derivatives.

$$\frac{\delta C}{\delta P^i} = \frac{\delta(w^L x^{i-1} + b^i)}{\delta P^i} \frac{\sigma[\delta(w^i x^{i-1} + b^i)]}{\delta(w^i x^{i-1} + b^i)} \frac{\delta C}{\sigma[\delta(w^i x^{i-1} + b^i)]}$$

- Where:

- $\delta C$  = Derivative of Cost Function
- $\delta P^i$  = Derivative of a Parameter, which could be the  $w^i$  weight or  $b^i$  bias or for activation function  $\delta(w^i x^{i-1} + b^i)$  at layer  $i$
- $x$  = Input Variable
- $\sigma$  = Activation Function (e.g. ReLU, Sigmoid)

(2.4)

Which when *equation: 2.2.3* is summed over all parameters of layer  $i$  becomes [2.5](#)

$$\nabla C = \frac{\delta C}{\delta P^i} = \sum^{n_i-1} \frac{\delta(w^L x^{i-1} + b^i)}{\delta P^i} \frac{\sigma[\delta(w^i x^{i-1} + b^i)]}{\delta(w^i x^{i-1} + b^i)} \frac{\delta C}{\sigma[\delta(w^i x^{i-1} + b^i)]} \quad (2.5)$$

Thus, taking the negative gradient  $-\nabla C$  will provide us gradient descent step hopefully towards the global minimum.

# *Data and Methodologies*

## **Data**

### **Raster pre-processing**

### **Data Augmentation**

Data augmentation is perhaps one of the most crucial task in training a robust neural-network. It is an economical way of increasing generalisability without increasing model complexity, data augmentation achieve this through, firstly increasing the quantity of training and validation data, secondly encompassing a greater range of textural, geometrical, and colour variability throught the creation of augmented pseudo-data (Shorten & Khoshgoftaar, 2019; Kinsley & Kukiela, 2020; Howard & Gugger, 2020; Zoph et al., 2019).

Data augmentation can generally be split into 3 categories: 1. Geometric/Affine distortion, 2. Colour distortion, and 4. Noise distortion. The application of which types of distortion to the *Train* and *Validation* dataset is highly dependent on the context of the semantic task. Therefore, care must be taken as to not introduce mislabelling (*see Figure 3.1*) (Ng A., 2018).

#### **Augmentation categories:**

- Geometric/Affine distortion
  - e.g. Fliping, Stretching, Rotation...
- Colour distortion
  - e.g. Colour Inversion, Solarise Colour, Greyscale...
- Noise distortion
  - e.g. Blurring, Contrasting, Salt & Pepper...

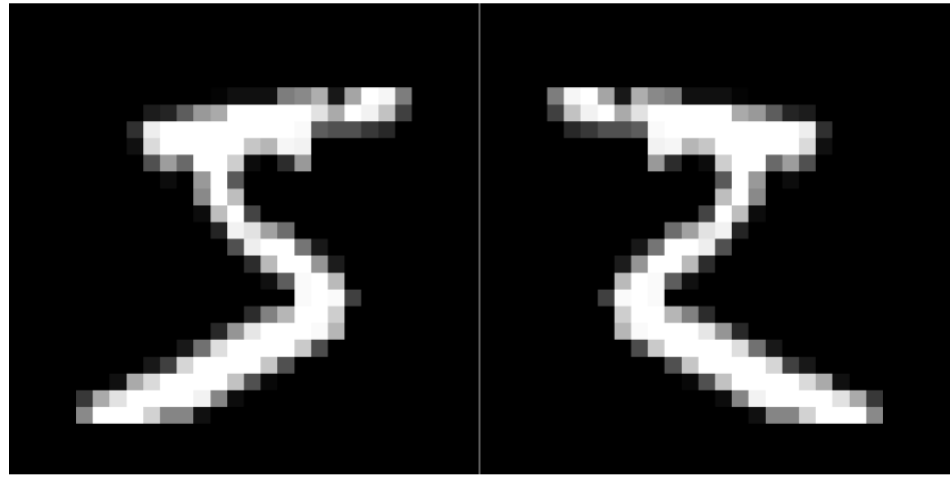


Figure 3.1: Perhaps geometric augmentation of horizontal flipping shall not be applied on the MNIST number of 5

## Research Questions and experiment design

In order to train a model which performs well on drone imagery, the motion artefact will be a significant feature for the model to learn. The combination of data availability have allow a unique set of research questions concerning the input data quality and experiment setup to surface.

1. RQ1: What is the optimal mixture of accurate and less-accurate labels and how does that affect the segmentation output result?
  - (a) How does the introduction of complex roofing materials affect result?
2. RQ2: Which is the best lightweight model given the limited data and computational resources for binary semantic segmentation?
  - (a) How does transfer learning from various initialised weights affect result?

Therefore, to test out U-Net and a few variation of the U-Net performance, an additional set of label data was created in order to supplement the imperfection in the labelled data of the Dzaleka camps. Initially, the models will be trained on the pixel-perfect and less complex Kalobeyei dataset, this will be then be followed by introducing the Dzaleka datasets of higher complexity. A comparison of baseline performance between the U-Net variations (Ronneberger et al., 2015) and the [Open-Cities-AI-Challenge \(OCC\)](#)

[winning model](#) is conducted. The baseline experiment aims to keep the hyperparameters (e.g. optimiser, learning rate, weight decay etc.) constant to obtain an objective view of the architectural responses on the same dataset setup. This will provide a clear picture of the feasibility and how to take this project further, so that further resources could be justified to scale future experiments.

## Architecture and hyperparameter selection

Model architecture and their associated hyperparameters selection is highly dependent on the computational resources and the task at hand (Ng A., 2018, Howard & Gugger, 2020). As this study aims to output a pixel-based binary segmentation which delineates building and non-building, and given the computational resources constraint, tried and tested architectures with relatively low number of training parameters is ideal.

### The U-Net and U-Net variants

The U-Net architecture was first developed by Ronneberger et al. (2015) for the task of cell segmentation in biomedical electronmicroscope images. The architecture feature a symmetrical Encoder-Decoder structure (*see figure ??*) and as with many other CNN, the architecture have transferred successfully well into the remote sensing domains (Höser & Künzer, 2020, Höser et al., 2020) (e.g. Jean et al., 2016, Xu et al., 2019)

### Pre-trained weights on Deep Learning models

Another major consideration of this study is to compare the performance of the architectures on various pre-trained weights. Due to the representation learning feature of CNN, studies have shown transfer learning on pre-trained weights even across different domain dataset could result in better performance, especially on projects with less data availability (LeCun et al., 2015, Zhu et al., 2017, Tan et al., 2018). Pre-trained weights for this study are ImageNet weights and the drone-based building segmentation competition (OCC) weights. Thus, one of the objective of this study is to find out whether transfer training performance on various pretrained weights would outperform training from scratch.

### EfficientNet encoders

## Accuracy Assessment

Detail and scrutible accuracy assessments are fundamental towards any classification based analysis. This section will introduce and break down the

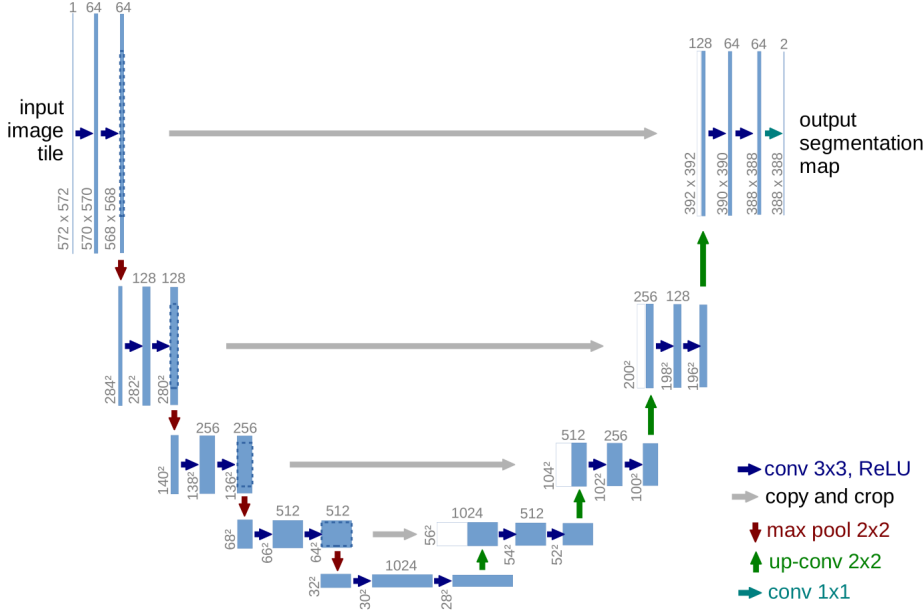


Figure 3.2: The Encoder-Decoder U-Net architecture (Ronneberger et al., 2015)

various lower order and higher order class-based (thematic) accuracy assessment. By explaining the characteristics of each metrics, this will provide a much more granular nature of accuracy assessment in the findings of section 4. In general, accuracy assessment in remote sensing can be divided into 2 categories: 1. Positional Accuracy & 2. Thematic Accuracy. Of which, Positional Accuracy deals with the accuracy of the location while Thematic Accuracy deals with the labels or attributes accuracy (Congalton & Green, 2019 & Bolstad, 2019). The rest of this section will consider the lower order and higher order accuracy metrics, with lower order metrics being more granular while higher order metrics more triturated but generalised.

The metrics described in this section form part of the larger family of accuracy assessment metrics that can be constructed from the confusion matrix (*see Figure 3.3*)

### Precision, Recall, Sensitivity, and Specificity

#### Precision, Recall, and Specificity

**Precision** and **Recall**, aka. Positive-Predictive-Value and Sensitivity/True-Positive-Rate Respectively. The two metrics are often used together, another common denomination especially in remote sensing literature are User's Ac-

		True condition		Prevalence $= \frac{\sum \text{Condition positive}}{\sum \text{Total population}}$	Accuracy (ACC) = $\frac{\sum \text{True positive} + \sum \text{True negative}}{\sum \text{Total population}}$
Total population		Condition positive	Condition negative		
Predicted condition	Predicted condition positive	True positive	False positive, Type I error	Positive predictive value (PPV), Precision = $\frac{\sum \text{True positive}}{\sum \text{Predicted condition positive}}$	False discovery rate (FDR) = $\frac{\sum \text{False positive}}{\sum \text{Predicted condition positive}}$
	Predicted condition negative	False negative, Type II error	True negative	False omission rate (FOR) = $\frac{\sum \text{False negative}}{\sum \text{Predicted condition negative}}$	Negative predictive value (NPV) = $\frac{\sum \text{True negative}}{\sum \text{Predicted condition negative}}$
	True positive rate (TPR), Recall, Sensitivity, probability of detection, Power = $\frac{\sum \text{True positive}}{\sum \text{Condition positive}}$	False positive rate (FPR), Fall-out, probability of false alarm = $\frac{\sum \text{False positive}}{\sum \text{Condition negative}}$	Positive likelihood ratio (LR+) = $\frac{\text{TPR}}{\text{FPR}}$	Diagnostic odds ratio (DOR) = $\frac{\text{LR+}}{\text{LR-}}$	F <sub>1</sub> score = $2 \cdot \frac{\text{Precision} \cdot \text{Recall}}{\text{Precision} + \text{Recall}}$
	False negative rate (FNR), Miss rate = $\frac{\sum \text{False negative}}{\sum \text{Condition positive}}$	Specificity (SPC), Selectivity, True negative rate (TNR) = $\frac{\sum \text{True negative}}{\sum \text{Condition negative}}$	Negative likelihood ratio (LR-) = $\frac{\text{FNR}}{\text{TNR}}$		

Figure 3.3: The Confusion Matrix

curacy and Producer's Accuracy (Congalton & Green, 2019 & Wegmann et al., 2016). To avoid further confusion in nomenclature, **Precision** and **Recall** will be used from hereon.

**Precision** is the measure of correctly predicted Positive class (True Positive) against all positive prediction assigned to that class (True Positive + False Positive) i.e. Given the predicted results, of those that are predicted as positive, what proportion were True. It can be expressed mathematically as:

$$\text{Precision} = \frac{\text{True Positive}}{(\text{True Positive} + \text{False Positive})} \quad (3.1)$$

Meanwhile, **Recall** measures the correctly predicted Positive class (True Positive) against both the correct and incorrect prediction on the Positive reference class (True Positive + False Negative) i.e. Given the predicted results, of those that are referenced as positive, what proportion of those were True. It can be expressed mathematically as:

$$\text{Recall} = \frac{\text{True Positive}}{(\text{True Positive} + \text{False Negative})} \quad (3.2)$$

**Specificity**, aka. True-Negative-Rate measures correctly predicted Negative class (True Negative) against the correct and incorrect prediction on the Negative reference class (False Positive + True Negative) i.e. Given the predicted results, of those that are referenced as negative, what proportion of those were True. It can be expressed mathematically as:

$$\text{Specificity} = \frac{\text{True Negative}}{(\text{False Positive} + \text{True Negative})} \quad (3.3)$$

Therefore, higher **Recall** suggests the model is better at identifying positives and vice-versa higher **Specificity** suggests the model is better at identifying negatives. Since this is an exercise that aim to maximise the positive prediction as a binary building segmentation classifier, emphasise will be placed on maximising **Precision** and **Recall**.

### Overall Accuracy, Dice Score, and Intersection-over-Union

### Experimentation setup

Each network architecture and their associated weights will be trained on 2 data setup. The first setup consist of only the Kalobeyei, Kakuma camp where the labels include drone motion artefacts and rooftops are relatively homogeneous. The second setup consist of data from the Kalobeyei camp and also the rest of Dzaleka, Dowa camp. The second setup will introduce imperfection in labelling and complex heterogeneous rooftops and morphologies. The two data setup will allow comparison between the models response of each class-based accuracy assessment metrics.

To truly assess the performance of the architecture output, a combination of the validation loss, class-based accuracy assessments, and

### Project workflow

## *Findings*

### Analysis

## *Discussion*

## *Conclusion*

## *Bibliography*

## *Appendix*